



MAX-PLANCK-GESELLSCHAFT

**Max Planck Institute Magdeburg  
Preprints**

Peter Benner

Jan Heiland

**LQG-Balanced Truncation  
Low-Order Controller  
for Stabilization of Laminar Flows**



MAX-PLANCK-INSTITUT  
FÜR DYNAMIK KOMPLEXER  
TECHNISCHER SYSTEME  
MAGDEBURG

## Abstract

Recent theoretical and simulation results have shown that Riccati based feedback can stabilize flows at moderate Reynolds numbers. We extend this established control setup by the method of *LQG-balanced truncation*. In view of practical implementation, we introduce a controller that bases only on outputs rather than on the full state of the system. Also, we provide a very low dimensional observer so that the control actuation can be computed in an online fashion.

## Contents

<b>1 Introduction</b>	<b>1</b>
<b>2 LQG-balanced Truncation for Low-Order Controller Design</b>	<b>2</b>
<b>3 LQG-balanced Truncation for Linearized Navier-Stokes Equations</b>	<b>5</b>
<b>4 Numerical Example</b>	<b>6</b>
<b>5 Conclusion</b>	<b>9</b>

### Impressum:

**Max Planck Institute for Dynamics of Complex Technical Systems, Magdeburg**

**Publisher:**

Max Planck Institute for  
Dynamics of Complex Technical Systems

**Address:**

Max Planck Institute for  
Dynamics of Complex Technical Systems  
Sandtorstr. 1  
39106 Magdeburg

<http://www.mpi-magdeburg.mpg.de/preprints/>

# 1 Introduction

The control of flows is of high interest in practical applications and a field of ongoing research [11, 12]. The particular aspect of stabilization of flows is of importance, for example, in technical flows where stable quasi-stationary working conditions are required.

We consider the generic control setup consisting of a plant, a controller that can act onto the plant, and a measurement or observation unit that delivers information on the current state of the plant. In the realm of flow control the plant may be modelled by semi-discrete Navier-Stokes equations for the evolution of the velocity  $v(t)$  and the pressure  $p(t)$  for time  $t > 0$  in an incompressible flow:

$$M\dot{v} = -N(v)v - \frac{1}{Re}Lv + J^T p + f, \quad (1)$$

$$0 = Jv - g, \quad (2)$$

$$v(0) = \alpha. \quad (3)$$

We assume, that the controller can act onto the system by changing certain components of the inhomogeneity  $f \leftarrow f + Bu$  in (1) and that the observations  $y$  are in a linear relation with  $v$ .

The well-understood approach of *open-loop control* [9] does not well apply for stabilization since it cannot react on perturbations. One rather resorts to *closed-loop control* where the controller decides on the current state information. Recent publications [3, 5] have reported successful applications of static state-feedback boundary control for the stabilization of flows at moderate Reynolds numbers in simulations. The presented approach employs low-rank Newton-ADI iterations [4] to solve for Riccati-based feedback gains and, thus, despite its generality, it is feasible for high-dimensional systems.

The novelties we propose are of practical impact. In view of a generic control setup, where the full state is generally not available, we consider a *Kalman observer* that determines the feedback control from a few measurements. Combined with the *LQG-balanced truncation* model reduction technique, we design a reduced controller of very low dimension, that can be evaluated in literally no time and, thus, is suitable for online feedback control.

To derive the low-order controller, we extend the method of *LQG-balanced truncation* [16] to the case of linearized Navier-Stokes equations. The DAE structure of the state equations (1-2) will be treated implicitly, as it was derived for the *Lyapunov equations* used in *balanced truncation* in [8] and as it was exploited for the solution *Riccati equations* in [2, 3]. Furthermore, since the controller acts only in the differential equation in (1), and since, though implicitly, we only consider the system that is projected onto the differential part, we do not need to account for an *improper* component of the system's transfer function as it was laid out in [6, 18]. For the same reasons, the relation of our work to [15] is only marginal. In particular, the choice of the actuation cannot make the system *impulse controllable*.

The paper is structured as follows. In Section 2, we introduce the method of *LQG-balanced truncation*. In view of implementation, we formulate the equations with the

presence of a mass matrix. In Section 3, we extend the theory and the equations to case of the linearized Navier-Stokes equations. To show applicability, we present a numerical example in Section 4. We conclude the paper by summarizing remarks on the potential impact and on the shortcomings of the presented results.

## 2 LQG-balanced Truncation for Low-Order Controller Design

We start with a review of known results for reduced-order controller synthesis by *LQG-balanced truncation*. For further reference, we illustrate basic system theoretic concepts and the derivation of a balanced system by an example problem.

Consider the linear time-invariant system

$$M\dot{v} = Av + Bu, \quad (4)$$

$$v(0) = 0, \quad (5)$$

$$y = Cv, \quad (6)$$

with matrices  $A, M \in \mathbb{R}^{n_v, n_v}$ ,  $B \in \mathbb{R}^{n_v, n_u}$ , and  $C \in \mathbb{R}^{n_y, n_v}$ , a state  $x(t) \in \mathbb{R}^{n_v}$ , an input  $u(t) \in \mathbb{R}^{n_u}$ , and an output  $y(t) \in \mathbb{R}^{n_y}$ . The mass matrix  $M$  is assumed to be symmetric and strictly positive definite.

We will call (4-6) a state space system that realizes a transfer function  $G: \mathcal{U} \rightarrow \mathcal{Y}$ , where  $\mathcal{U}$  and  $\mathcal{Y}$  denote the spaces of inputs and outputs, respectively. We will frequently write  $G = (M, A, B, C, D)$ .

We recall that a transfer function has infinitely many realizations. Particularly, for invertible transformation matrices  $\mathcal{W} \in \mathbb{R}^{n_v, n_v}$  and  $\mathcal{V} \in \mathbb{R}^{n_y, n_y}$  one has that

$$G = (M, A, B, C, D) \text{ equals } \tilde{G} = (\mathcal{W}^T M \mathcal{V}, \mathcal{W}^T A \mathcal{V}, \mathcal{W}^T B, C \mathcal{V}), \quad (7)$$

in the sense that  $G$  and  $\tilde{G}$  map the same inputs  $u$  onto the same outputs  $y$ . Among the realizations, *minimal realizations* are those for which the state  $v$  has minimal dimension. For a *minimal realization*, one has the following characteristic properties, cf. standard textbooks like [13] for a thorough introduction on the LQG control problem or [16] for an overview directed to the LQG-balanced truncation setup.

**Proposition 1** (cf. [16], Prop. 3.3). *Let  $G = (M, A, B, C)$  be minimal. Then there exists a unique symmetric positive definite stabilizing solution  $X_c \in \mathbb{R}^{n_v, n_v}$  to the control algebraic Riccati equation (CARE)*

$$A^T X_c M + M X_c A - M X_c B B^T X_c M + C^T C = 0 \quad (8)$$

*and there exists a unique symmetric positive definite stabilizing solution  $X_o \in \mathbb{R}^{n_v, n_v}$  to the filter algebraic Riccati equation (FARE)*

$$A X_o M + M X_o A^T - M X_o C^T C X_o M + B B^T = 0. \quad (9)$$

Then the LQG regulator is given via the control law

$$u = -B^T M X_c \hat{x}, \quad (10)$$

where  $\hat{x}$  is the state of the Kalman observer

$$M \dot{\hat{x}} = (A - X_o M C^T C - B B^T X_c M) \hat{x} + X_o M C^T y. \quad (11)$$

Equations (8-11) are derived from the standard case with  $M = I$  through a scaling of (4) by  $M^{-1}$  and redefining  $X_c \leftarrow M^{-1} X_c M^{-1}$  and  $X_o \leftarrow M^{-1} X_o M^{-1}$ .

In the pioneering work [10] it was found that for minimal realizations the eigenvalues of the product of the solutions of the CARE and FARE are invariant under equivalence transformations of the system. Then, as in the case of *balanced truncation*, cf. [1], balanced realizations can be defined, interpreted, and truncated. We adapt the results and arguments given in [16] to the case with a mass matrix  $M$ .

**Proposition 2** (cf. [16], Prop. 3.4). *Let  $G = (M, A, B, C)$  be minimal and let  $X_c$  and  $X_o$  be the unique symmetric positive definite stabilizing solution to the CARE and FARE, respectively. Consider transformations as in (7) with regular matrices  $\mathcal{W}$  and  $\mathcal{V}$  with  $\mathcal{W}^T M \mathcal{V} = I$ . Then,*

- the unique symmetric positive definite stabilizing solutions  $\tilde{X}_c$  and  $\tilde{X}_o$  to the CARE and FARE associated with the transformed system  $\tilde{G}$  fulfill

$$\tilde{X}_c = \mathcal{V}^T M X_c M \mathcal{V} \text{ and } \tilde{X}_o = \mathcal{W}^T M X_o M \mathcal{W} \quad (12)$$

- and  $X_c M X_o$  and  $\tilde{X}_c \tilde{X}_o$  have the same eigenvalues.

*Remark 1.* Because of  $I = \mathcal{W}^T M \mathcal{V}$  the relations in (12) are the same as the commonly used relations

$$\tilde{X}_c = \mathcal{W}^{-1} X_c \mathcal{W}^{-T} \text{ and } \tilde{X}_o = \mathcal{W}^T M X_o M \mathcal{W}, \quad (13)$$

cf., e.g., [1, Ch. 4.3] for the balanced truncation case with  $M = I$ . In view of model reduction, for which we will apply non square transformations  $\mathcal{W}$  and  $\mathcal{V}$ , we will stay with formulation (12).

From the positive definiteness of the matrices  $M$ ,  $X_c$ , and  $X_o$ , it follows that the eigenvalues  $\{\mu_i^2\}_{i=1}^{n_v}$  of  $X_c M X_o$  are real and positive. Because of their invariance properties they are called *LQG-characteristic values* [16].

Furthermore, there exist transformation matrices  $\mathcal{W}$ ,  $\mathcal{V}$ , with  $\mathcal{W}^T M \mathcal{V} = I$  such that for the solutions of  $\tilde{X}_c$ ,  $\tilde{X}_o$  of the AREs associated with the transformed  $\tilde{G} = (I, \mathcal{W}^T A \mathcal{V}, \mathcal{W}^T B, C \mathcal{V})$  it holds that

$$\tilde{X}_c = \tilde{X}_o = S, \quad (14)$$

where  $S$  is the diagonal matrix of the LQG characteristic values  $\{\mu_i\}_{i=1}^{n_v}$  in descending order. In line with the notion for *balanced truncation*, this realization of  $G$  is called *balanced realization*.

If one has factored the matrices  $X_c = U U^T$  and  $X_o = L L^T$  of any minimal realization, one can compute the transformations  $\mathcal{W}$  and  $\mathcal{V}$ , that realize (14), as follows:

Algorithm 1.

1. Compute a *Singular Value Decomposition* of  $U^T M L = Z S Y^T$ .
2. Set  $\mathcal{W} := U Z S^{-1/2}$  and  $\mathcal{V} = L Y S^{-1/2}$ .

With  $\mathcal{W}$  and  $\mathcal{V}$  chosen by Algorithm 1 we directly confirm that

$$\mathcal{W}^T M \mathcal{V} = S^{-1/2} Z^T U^T M L Y S^{-1/2} = S^{-1/2} Z^T Z S Y^T Y S^{-1/2} = I \quad (15)$$

and with (14) that

$$\tilde{X}_c = \mathcal{V}^T M X_c M \mathcal{V} = S^{-1/2} Y^T L^T M U U^T M L Y S^{-1/2} = S \quad (16)$$

and that

$$\tilde{X}_o = \mathcal{W}^T M X_o M \mathcal{W} = S^{-1/2} Z^T U^T M L L^T M U Z S^{-1/2} = S. \quad (17)$$

Thus, the singular values in  $S$  from Algorithm 1 are the LQG-characteristic values. Following [10], we interpret small values in  $S$  as associated with states in the balanced realization that are both difficult to control and to observe.

Consequently, if in Algorithm 1 we set

$$\mathcal{W} = \mathcal{W}_k := L Y_k S_k^{-1/2} \quad \text{and} \quad \mathcal{V} = \mathcal{V}_k = U Z_k S_k^{-1/2}, \quad (18)$$

where  $S_k$ ,  $Y_k$ , and  $Z_k$  are the submatrices of  $S$ ,  $Y$ , and  $Z$  that correspond to the  $n_k$  largest singular values, we can define a truncated system as

$$\tilde{G}_k = (\mathcal{W}_k^T M \mathcal{V}_k, \mathcal{W}_k^T A \mathcal{V}_k, \mathcal{W}_k^T B, C \mathcal{V}_k) =: (I_k, A_k, B_k, C_k). \quad (19)$$

With similar arguments as in (16) and (17), one confirms that

$$\tilde{X}_{c_k} := \mathcal{V}_k^T M X_c M \mathcal{V}_k = S_k \quad \text{and} \quad \tilde{X}_{o_k} = \mathcal{W}_k^T M X_o M \mathcal{W}_k = S_k. \quad (20)$$

Also, one can prove that  $\tilde{X}_{o_k}$  and  $\tilde{X}_{c_k}$  are the unique stabilizing solutions of the CARE and FARE for the truncated system  $\tilde{G}_k$  [16, Rem. 3.7].

Finally, we define a truncation of the controller defined in (10) and (11) via

$$u = -B_k^T \tilde{X}_{c_k} \hat{x}_k, \quad (21)$$

and the reduced observer

$$\dot{\hat{x}}_k = (A_k - \tilde{X}_{o_k} C_k^T C_k - B_k B_k^T \tilde{X}_{c_k}) \hat{x}_k + \tilde{X}_{o_k} C_k^T y_k, \quad (22)$$

which is the *Kalman* observer of the system  $\tilde{G}_k$ , cf. [16].

*Remark 2.* Although the analysis requires that the considered realization is minimal, the derived algorithms also work for general realizations. In what follows we will simply apply *LQG balanced truncation* to state space systems with unobservable and uncontrollable states, i.e. to systems that are not minimal. We will only require that the formally stated CARE and FARE uniquely define positive (semi-)definite solutions. Then, the fitness of the reduced model has to be checked in a post processing step.

Apart from the objections discussed in Remark 2, the *LQG balanced truncation* approach perfectly applies to large-scale cases, where low rank factors  $U_k$  and  $L_k$  that approximate  $X_c \approx U_k U_k^T$  and  $X_o \approx L_k L_k^T$  are computed. In such cases, Algorithm 1 readily provides truncating transformation matrices  $\mathcal{W}_k$  and  $\mathcal{V}_k$ .

### 3 LQG-balanced Truncation for Linearized Navier-Stokes Equations

We consider the semi-discrete Navier-Stokes equations modelling the evolution of the velocity  $v$  and the pressure  $p$  in an incompressible flow,

$$M\dot{v} = -N(v)v - \frac{1}{Re}Lv + J^T p + Bu + f \quad (23)$$

$$0 = Jv - g \quad (24)$$

$$v(0) = \alpha \quad (25)$$

$$y = Cv \quad (26)$$

starting from an initial state  $\alpha$ .

Systems as (23-26) arise, e.g., in a finite element discretization of a flow problem with distributed control and observation. Here  $M$  is the symmetric strictly positive mass matrix,  $L$  is the discretized Laplacian, and  $N(v)$  accounts for the convection that is linear in  $v$ . The discrete divergence operator is given by  $J$  and the discrete gradient by  $J^T$ . The control and the observation are modelled with the matrices  $B$  and  $C$ .

We assume that  $J$  is of full rank, i.e. the pressure  $p$  has been fixed to a certain level. Also we assume, that the source terms  $f$  and  $g$  in (23) and (24) only contain the boundary conditions and, thus, are constant in time.

Assume that  $\alpha$  is a steady state solution to (23-25) and write the unsteady solution as  $v = \alpha + v_\delta$  with a deviation  $v_\delta$  that we assume to be small. Then, neglecting the quadratic term in  $v_\delta$ , from Equations (23-26) we derive a linear model for the deviation in the output caused by the actuation  $Bu$ :

$$M\dot{v}_\delta = Av_\delta + J^T p + Bu \quad (27)$$

$$0 = Jv_\delta \quad (28)$$

$$v_\delta(0) = 0 \quad (29)$$

$$y_\delta = Cv_\delta, \quad (30)$$

where  $Av_\delta := -N(v_\delta)\alpha - N(\alpha)v_\delta - \frac{1}{Re}Lv_\delta$ .

Because of the constraint  $Jv_\delta = 0$ , the formulas of Section 2 do not simply apply. Therefore, we reformulate System (27-30) in terms of the *underlying ODE* that describes the motion of the parts of  $v_\delta$  that are not seen by the constraint. We point out, that the following algebraic manipulations are purely for extending the *LQG-balanced truncation* framework to the projected equations. Once we have arrived at the CARE (8) and FARE (9), we give references to a solution approach that avoids the numerically unfeasible computation of projectors.

Recall that  $M$  is symmetric strictly positive definite and that  $J$  is of full rank. Thus, we can define the projector

$$\mathcal{P} := I - M^{-1}J(J^T M^{-1}J)^{-1}J \quad (31)$$

that comes with the following properties:

**Proposition 3.** Consider System (27-30), let  $v_\delta$  be a solution to it, and let  $\mathcal{P}$  be defined as in (31). Then,

$$(a) \quad v_\delta(t) = \mathcal{P}v_\delta(t),$$

$$(b) \quad \mathcal{P}^T J^T p(t) = 0, \text{ for all time } t > 0, \text{ and}$$

$$(c) \quad \mathcal{P}^T M = M\mathcal{P}.$$

Using the relations of Proposition 3, we can state that  $v_\delta$  is a solution to (27-30) if, and only if, it solves

$$M\dot{v}_\delta = \mathcal{P}^T A v_\delta + \mathcal{P}^T B u \quad (32)$$

$$v_\delta(0) = 0 \quad (33)$$

$$y_\delta = C v_\delta. \quad (34)$$

For System (32-34), the CARE (8) and the FARE (9) write as

$$A^T \mathcal{P}^T X_c M + M X_c \mathcal{P} A - M X_c \mathcal{P} B B^T \mathcal{P}^T X_c M + C^T C = 0 \quad (35)$$

and

$$\mathcal{P} A X_o M + M X_o A^T \mathcal{P}^T - M X_o C^T C X_o M + \mathcal{P} B B^T \mathcal{P}^T = 0. \quad (36)$$

Low-rank factors approximating the solutions to Equations (35) and (36) can be obtained efficiently by combining *low-rank Newton-ADI* iterations [4] with the ideas of [8] that realize the application of  $\mathcal{P}$  in an implicit fashion. See, in particular, the references [2, 3, 5], where Equation (35) is solved to define a stabilizing feedback for flow problems.

*Remark 3.* By construction, cf. [8], the resulting transformation matrix  $\mathcal{W}_k$  fulfills  $\mathcal{W}_k = \mathcal{W}_k \mathcal{P}^T$ . Thus, a reduced system to (27-30),

$$\tilde{\mathcal{G}}_k = (I_k, A_k, B_k, C_k) := (\mathcal{W}_k^T M \mathcal{V}_k, \mathcal{W}_k^T A \mathcal{V}_k, \mathcal{W}_k^T B, C \mathcal{V}_k),$$

can be obtained without resorting the reformulation (32-34).

## 4 Numerical Example

Motivated by abstract results from [17], the authors of [2, 3] considered *LQ regulators* for a linearization of the flow-equations about a stationary solution  $\alpha$ . It turned out that the linear feedback may well be applied in the nonlinear equations to keep the flow quasi-stationary around  $\alpha$ .

To illustrate the applicability of *LQG-balanced truncation* based low-order controllers in the stabilization of unsteady flows, we consider the two-dimensional cylinder wake with distributed control and observation, as depicted in Figure 1. As the computational domain we consider the rectangle  $[0, 2.2] \times [0, 0.41]$  with the cylinder of radius 0.05 centered at (0.2, 0.2). The spatial coordinates we denote by  $x_1$  and  $x_2$ . The results

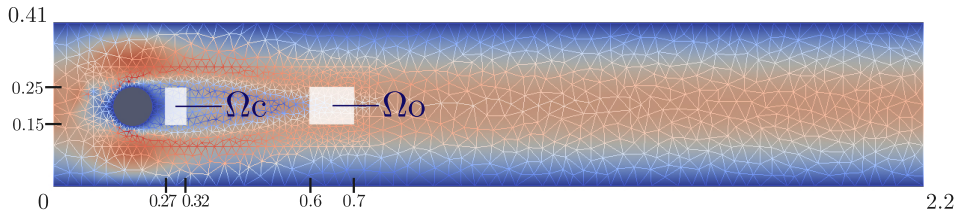


Figure 1: Setup of the 2D cylinder wake with control distributed in  $\Omega_C$  and observation distributed in  $\Omega_O$

presented are for *Reynolds number*  $Re = 133$ , calculated with the peak inflow velocity and the cylinder diameter.

As boundary conditions for the velocities, we impose a parabolic inflow profile at the left boundary and *no-slip* conditions on the top and the bottom wall. At the outflow, we employ *do-nothing* conditions.

The implementation was done in Python [7]. For the spatial discretization we used the Python interface *dolfin* to *FeNiCS* [14].

The spatial discretization was realized with a nonuniform triangulation of the computational domain and *Taylor-Hood* finite elements [19]. The considered discretization resulted in  $n_v = 9356$  and  $n_p = 1288$ .

For  $n_u \in \mathbb{N}$ , we set the input space  $\mathcal{U} := \mathcal{C}(0, T; U \times U)$ , where  $U$  is spanned by  $n_u$  linear hat functions equally distributed on the unit interval  $[0, 1]$ .

We define the domain of control to be  $\Omega_c = [0.27, 0.32] \times [0.15, 0.25]$ , cf. Figure 1, and the input operator  $B: \mathcal{U} \rightarrow \mathcal{C}(0, T; \mathcal{C}(\Omega; \mathbb{R}^2))$  via

$$B_1 u(t; x_1, x_2) = \begin{cases} \begin{bmatrix} u_1(t; \theta(x_1)) \\ u_2(t; \theta(x_1)) \end{bmatrix}, & \text{if } (x_1, x_2) \in \Omega_c, \\ 0, & \text{elsewhere,} \end{cases} \quad (37)$$

with the affine linear function  $\theta_c$  mapping  $[0.27, 0.32]$  onto  $[0, 1]$ .

For  $n_y$ , we define the output space  $\mathcal{Y}$  similar to  $\mathcal{U}$ . As the domain of observation, we use  $\Omega_o = [0.6, 0.7] \times [0.15, 0.25]$ , cf. Figure 1, and for a  $v \in \mathcal{C}(0, T; \mathcal{C}(\Omega; \mathbb{R}^2))$ , we define the observation operator  $C: v \rightarrow y \in \mathcal{Y}$  via

$$Cv(t)(\eta) = \begin{bmatrix} y_{x_1}(t; \eta) \\ y_{x_2}(t; \eta) \end{bmatrix} = \int_{0.6}^{0.7} \mathcal{P}_{\mathcal{Y}} \begin{bmatrix} v_1(t; x_1, \theta_o(\eta)) \\ v_2(t; x_1, \theta_o(\eta)) \end{bmatrix} dx_1, \quad (38)$$

where  $\theta_o$  is an affine linear mapping adjusting  $[0, 1]$  to  $[0.15, 0.25]$  and where the projector to the finite dimensional subspace  $\mathcal{P}_{\mathcal{Y}}: [L^2(0, 1)]^2 \rightarrow Y \times Y$  is chosen as the orthogonal  $L^2$  projection.

By definition,  $C$  is defined such that it measures the velocity  $v(t)$  in  $\Omega_o$  averaged in  $x_1$  direction. The  $x_2$ -dependence is approximated by  $n_y$  basis functions of  $Y$ . The

$\kappa$	$n_k$	$d_k$
$10^{-4}$	42	0.01803696
$10^{-3}$	22	0.01803715
$10^{-2}$	13	0.01804118
$10^{-1}$	4	0.01818847
$10^{-0}$	2	3.16595044

Table 1: Dimension  $n_k$  of the reduced system for varying thresholds  $\kappa$  and the integrated deviation from the target output  $d_k := \int_0^{12} \|y_k(t) - y_\alpha\|_2 dt$ .

input operator  $B$  maps the input into  $\Omega_c$  such that it is constant in  $x_1$  direction and space-varying in  $x_2$ .

In the semi-discrete setting  $v$  is typically assumed in a finite dimensional, continuous space over  $\Omega$ . By standard results, for continuous inputs, a solution  $v$  of (23-25) is continuous in time on its interval of existence. Thus, the choice of the input and output spaces and operators are justified.

In the presented examples we have chosen  $n_u = n_y = 3$ , meaning that the  $x_1$  and  $x_2$  components of both input and output signal are described by 3 nodal values each.

We set  $\alpha$  to be the steady-state solution and consider the linearized system as in (27-30). Then we compute low-rank factors  $U_k$  and  $L_k$  that approximate the solutions to the projected CARE (35) and the projected FARE (36),  $X_c \approx U_k U_k^T$  and  $X_o \approx L_k L_k^T$ , using the methodology described in [2]. As stabilizing initial guesses, we used solutions for lower *Reynolds numbers*. From the factors we compute  $\mathcal{W}_k$  and  $\mathcal{V}_k$  as defined in Equation (18) and the reduced system as  $\tilde{G}_k = (I_k, A_k, B_k, C_k)$ , cf. Remark 3.

For varying thresholds  $\kappa$ , we cut-off all *LQG-characteristic values*  $\mu_i < \kappa$ , to get reduced systems of various size, see Table 1.

The reduced systems  $\tilde{G}_k$  give good approximations to the linearized equations (27-30) both in in frequency (Figure 3) and time domain (Figure 2). Clearly, the reduced (linear) system cannot reproduce the nonlinear dynamics (Figure 2(b)).

However, the reduced controller, as defined via Equations (19), (21), and (22), well stabilizes the closed-loop system:

$$M\dot{v} = -N(v)v - \frac{1}{Re}Lv + J^T p - BB_k^T \tilde{X}_{ck} \hat{x}_k + f, \quad (39)$$

$$0 = Jv - g, \quad (40)$$

$$v(0) = \alpha, \quad (41)$$

$$y_k = Cv, \quad (42)$$

$$\dot{\hat{x}}_k = (A_k - \tilde{X}_{ok} C_k^T C_k - B_k B_k^T \tilde{X}_{ck}) \hat{x}_k + \tilde{X}_{ok} C_k^T (y_k - y_\alpha), \quad (43)$$

where  $\alpha$  is the steady-state solution and  $y_\alpha := C\alpha$ .

For numerical testing, we integrated the nonlinear closed-loop system starting from  $v(0) = \alpha + \epsilon$ , where  $\epsilon := 10^{-3} \mathcal{P} \mathbf{e}$  and  $\mathbf{e} \in \mathbb{R}^{n_v}$  is the vector of ones. The perturbation

$\epsilon$  was introduced to trigger the instabilities. We considered the time interval  $(0, T]$  discretized by a constant time step of length 0.005. As the numerical integration scheme for the state equations (39-40) we used the trapezoidal rule with an explicit treatment of the nonlinear part. The observer equation (43) was numerically integrated using the *implicit Euler* scheme. The control was lagged by one time-step, so that the current input was computed from the measurements of the previous states.

As can be seen from Figure 4, plotting the measurement signal  $y(t)$  versus the time, the uncontrolled system is unstable and soon attains a state of periodic fluctuations. This is characteristic for the cylinder wake at moderate Reynolds numbers. If the loop is closed, the system stays in a quasi stationary state (Figure 4(a)). Also, see Figure 5 for a plot of the deviation of the output from the starting value for different orders of reduction. We want to point out that the flow field was indeed stabilized, see Figure 6 for snapshots of the stabilized and the uncontrolled velocity fields.

*Remark 4.* Note that the feedback control is defined only by the current output. Furthermore, the estimated state  $\hat{x}_k(t)$  is obtained via the solution of an observer system of reduced dimension. In the presented example, a reduced system of order  $n_k = 4$  has been enough for stabilization, cf. Table 1 and Figure 5. Recalling that the observer (43) is a linear time-invariant system, for a constant time-step length, all factors for the chosen numerical integration scheme can be precomputed. Thus, the effort for the update of  $\hat{x}_k$  reduces to two small matrix-vector multiplications.

## 5 Conclusion

We have provided a generalization of *LQG-balanced truncation* to the setup of flow equations. We have shown that recent results on projected low-rank Newton-ADI iterations can also be applied here, what makes the approach feasible for very general large-scale problems. The presented numerical example illustrates the potential of *LQG-balanced truncation* for stabilization of flows. Particularly, we could stabilize the cylinder wake by a very low-order controller that only considers a low-dimensional output. We have argued, that this controller is capable of online-control in physical setups.

A shortcoming of the presented theory is the assumption that the control acts distributed in space, what is difficult to realize in a control setup. One task for future work will be to adapt the results of [3, 5], that stabilize the cylinder via boundary control, to the reduced controller setup.

## References

- [1] A. C. Antoulas. *Approximation of Large-Scale Dynamical Systems*. SIAM Publications, Philadelphia, PA, 2005.
- [2] E. Bänsch and P. Benner. Stabilization of incompressible flow problems by Riccati-based feedback. In G. Leugering, S. Engell, A. Griewank, M. Hinze, R. Rannacher,

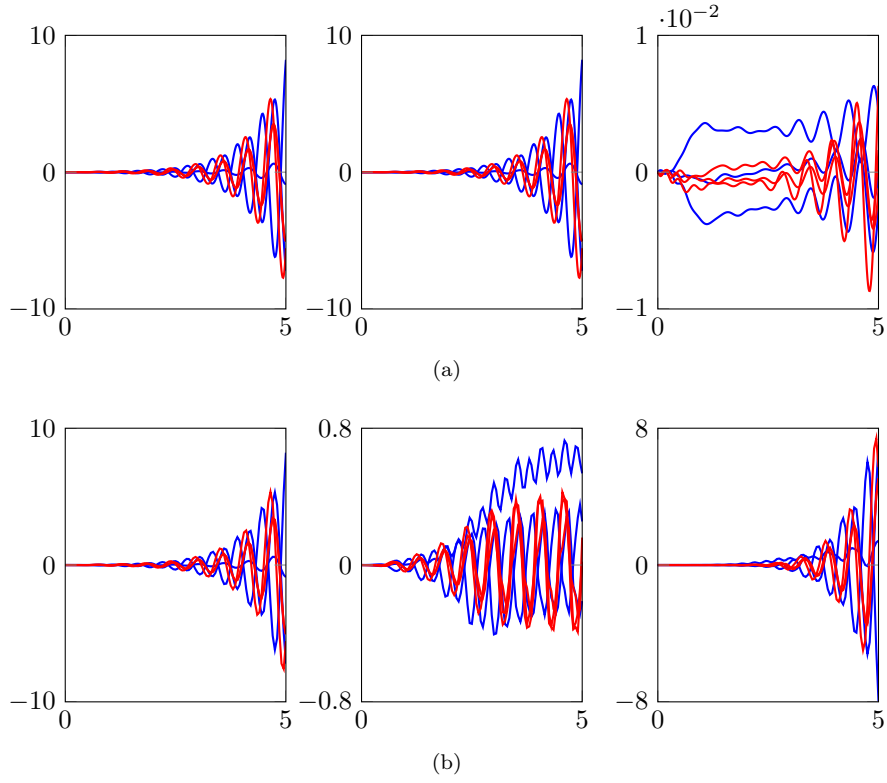


Figure 2: Step response for one input component for  $t \in [0, 5]$ . The left column shows the response  $y_k(t) - y_\alpha$  of the reduced system of dimension  $n_k = 13$ . The middle column shows the response  $y(t) - y_\alpha$  of the full system ( $n_v = 9356$ ), and the right column the difference. Here,  $y_\alpha$  is the output of the linearization point. The (unstable) linearized system is well approximated (a), unlike the nonlinear system (b). The blue lines depict the  $x_1$ -components of  $y(t)$  and the red lines correspond to the  $x_2$ -components of  $y(t)$ .

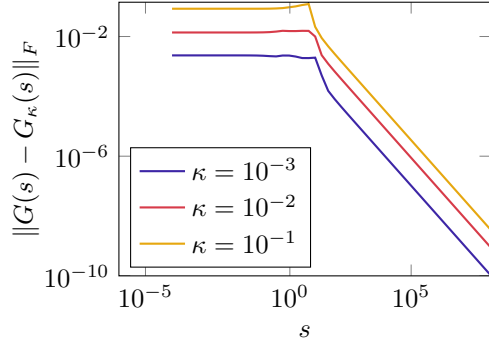


Figure 3: The error in the frequency response for varying thresholds  $\kappa$ .

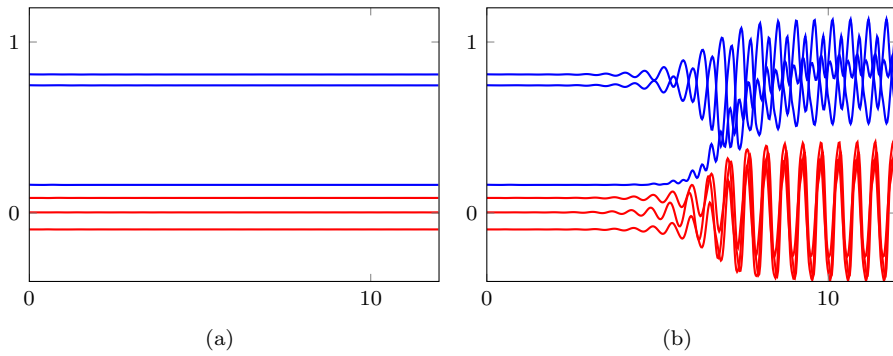


Figure 4: The measured signal  $y_k$  over time  $t \in [0, 12]$  of the closed loop system (a) with a reduced controller of dimension  $n_k = 13$ , compared to the response of the uncontrolled system (b). The blue lines depict the  $x_1$ -components of  $y(t)$  and the red lines correspond to the  $x_2$ -components of  $y(t)$ .

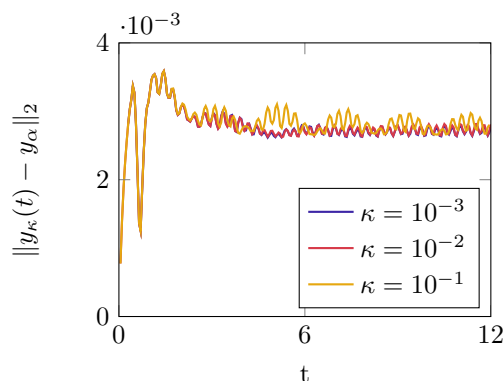
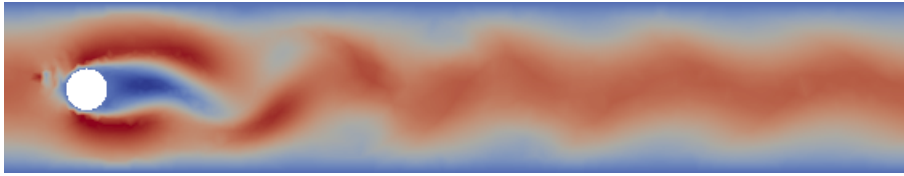


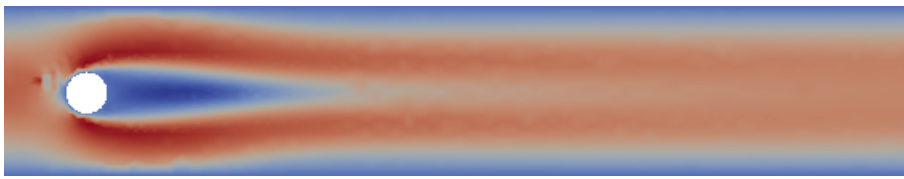
Figure 5: The deviation of the measured output  $y_k$  from the steady-state output  $y_\alpha$  for varying thresholds  $\kappa$ .

V. Schulz, M. Ulbrich, and S. Ulbrich, editors, *Constrained Optimization and Optimal Control for Partial Differential Equations*, volume 160 of *International Series of Numerical Mathematics*, pages 5–20. Birkhäuser, 2012.

- [3] E. Bänsch, P. Benner, J. Saak, and H. K. Weichelt. Riccati-based boundary feedback stabilization of incompressible Navier-Stokes flow. Preprint SPP1253-154, DFG-SPP1253, 2013.
- [4] P. Benner, J.-R. Li, and T. Penzl. Numerical solution of large Lyapunov equations, Riccati equations, and linear-quadratic control problems. *Numer. Lin. Alg. Appl.*, 15(9):755–777, 2008.
- [5] P. Benner, J. Saak, M. Stoll, and H. Weichelt. Efficient solution of large-scale saddle point systems arising in Riccati-based boundary feedback stabilization of incompressible Stokes flow. *SIAM J. Sci. Comput.*, 35(5):S150–S170, 2013. Early version as SPP1253 Preprint: <http://www.am.uni-erlangen.de/home/spp1253/wiki/images/b/bc/Preprint-SPP1253-130.pdf>.
- [6] S. Gugercin, T. Stykel, and S. Wyatt. Model reduction of descriptor systems by interpolatory projection methods. *SIAM J. Sci. Comput.*, 35(5):B1010B1033, 2013.
- [7] J. Heiland. lqgbt-oseen - python module for lqgbt of linearized flow equations. <https://github.com/highlando/lqgbt-oseen>, 2014.
- [8] M. Heinkenschloss, D. C. Sorensen, and K. Sun. Balanced truncation model reduction for a class of descriptor systems with applications to the Oseen equations. *SIAM J. Sci. Comput.*, 30(2):1038–1063, 2008.
- [9] M. Hinze and K. Kunisch. Second order methods for optimal control of time-dependent fluid flow. *SIAM J. Control Optim.*, 40(3):925–946, 2001.



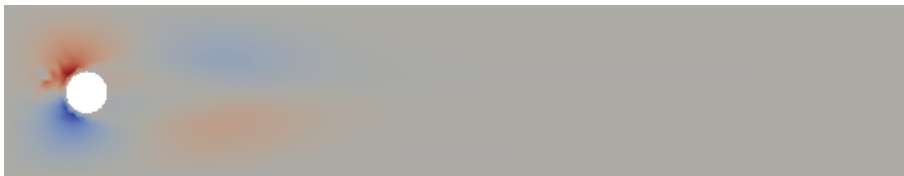
(a)



(b)



(c)



(d)

Figure 6: Snapshots at  $t = 12$  of the  $x_1$  and  $x_2$  components of the velocity in case uncontrolled case (a) and (c) and in the closed-loop case (b) and (d) with  $\kappa = 10^{-2}$ , respectively.

- [10] E. A. Jonckheere and L. M. Silverman. A new set of invariants for linear systems – application to reduced order compensator design. *IEEE Trans. Automat. Control*, 28:953–964, 1983.
- [11] R. King (editor). *Active flow control. Papers contributed to the conference ‘Active flow control 2006’, Berlin, Germany, September 27–29, 2006*. Springer, Berlin, Germany, 2007.
- [12] R. King (editor). *Active Flow Control II: Papers Contributed to the Conference ‘Active Flow Control II 2010’, Berlin, Germany, May 26 to 28, 2010*. Notes on Numerical Fluid Mechanics and Multidisciplinary Design. Springer, 2010.
- [13] A. Locatelli. *Optimal Control: An Introduction*. Birkhäuser, Basel, Boston, Berlin, 2001.
- [14] A. Logg, K. B. Ølgaard, M. E. Rognes, and G. N. Wells. FFC: the FEniCS form compiler. In *Automated Solution of Differential Equations by the Finite Element Method*, pages 227–238. Springer-Verlag, Berlin, Germany, 2012.
- [15] J. Möckel, T. Reis, and T. Stykel. Linear-quadratic gaussian balancing for model reduction of differential-algebraic systems. *Internat. J. Control*, 84(10):1627–1643, 2011.
- [16] D. Mustafa and K. Glover. Controller design by  $\mathcal{H}_\infty$ -balanced truncation. *IEEE Trans. Automat. Control*, 36(6):668–682, 1991.
- [17] J.-P. Raymond. Local boundary feedback stabilization of the Navier-Stokes equations. In *Control Systems: Theory, Numerics and Applications, Rome, 30 March – 1 April 2005*, Proceedings of Science. SISSA, <http://pos.sissa.it>, 2005.
- [18] T. Stykel. Balanced truncation model reduction for semidiscretized Stokes equation. *Linear Algebra Appl.*, 415(2–3):262–289, 2006.
- [19] C. Taylor and P. Hood. A numerical solution of the Navier-Stokes equations using the finite element technique. *Internat. J. Comput. & Fluids*, 1(1):73–100, 1973.

